Supporting Information

Efficient photonic materials based on Ni bis(dithiolene) fused with benzene, having gigantic second hyper polarizabilities. A computational study

Aggelos Avramopoulos,[a,b*] Nicolás Otero,[c,d] Heribert Reis,[a] Panaghiotis Karamanis,[c] Manthos G. Papadopoulos [a*]

[a] Institute of Biology, Pharmaceutical Chemistry and Biotechnology, National Hellenic Research Foundation, 48 Vas. Constantinou Ave., Athens 11635, Greece.

[b] Department of Computer Engineering, Technological Education Institute (TEI) of Sterea Ellada, Lamia 35100, Greece

[c] CNRS/ UNIV Pau & Pays Adour, Institut Des Sciences Analytiques et de Physico-Chimie pour l'environnement et les Materiaux MIRA*, UMR5254, 64000, Pau, France. Hlioparc Pau Pyrnes 2 avenue du Prsident Angot, 64053 PAU Cedex 09 France.

[d] Departamento de Química Física, Universidade de Vigo,36310, Vigo, Galicia, Spain

* Corresponding Authors: aavram@eie.gr (AA), mpapad@eie.gr (MGP)

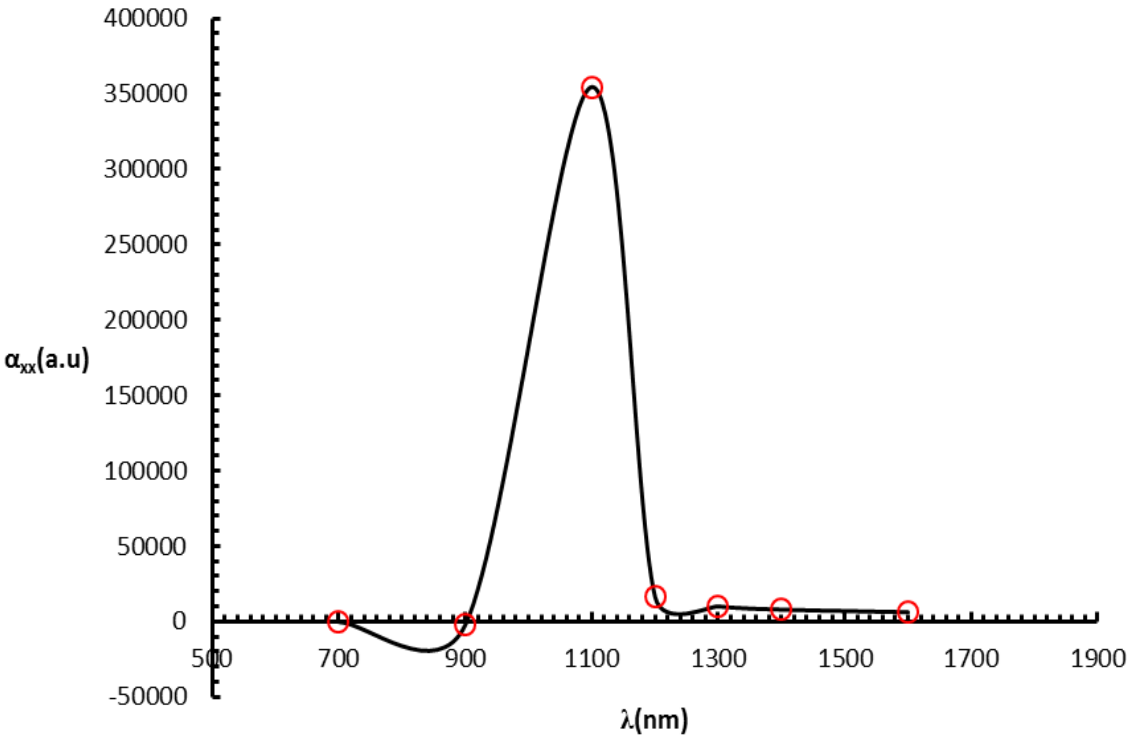

Figure S1. The variation of the polarizability of $(B\text{-}NiBDT)_3$ derivative with the wavelength. All the values were computed with (U)CAM-B3LYP/6-31G* method.

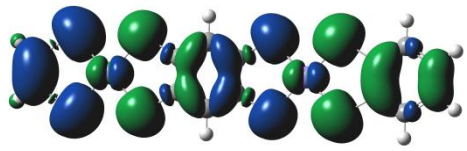

n=2

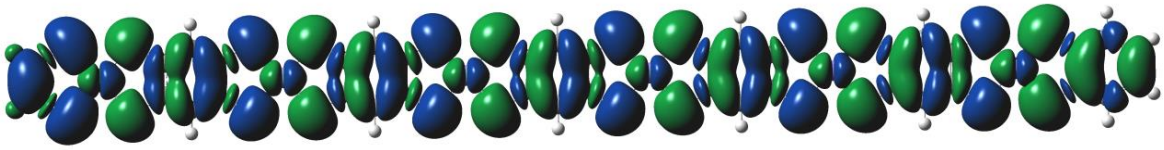

n=6

Figure S2. Spin densities for $(NiBDT\text{-}B)_n$,n=2,6 derivatives, computed with (U)B3LYP/6-31G*. Blue and green lobes depict positive and negative regions, respectively.

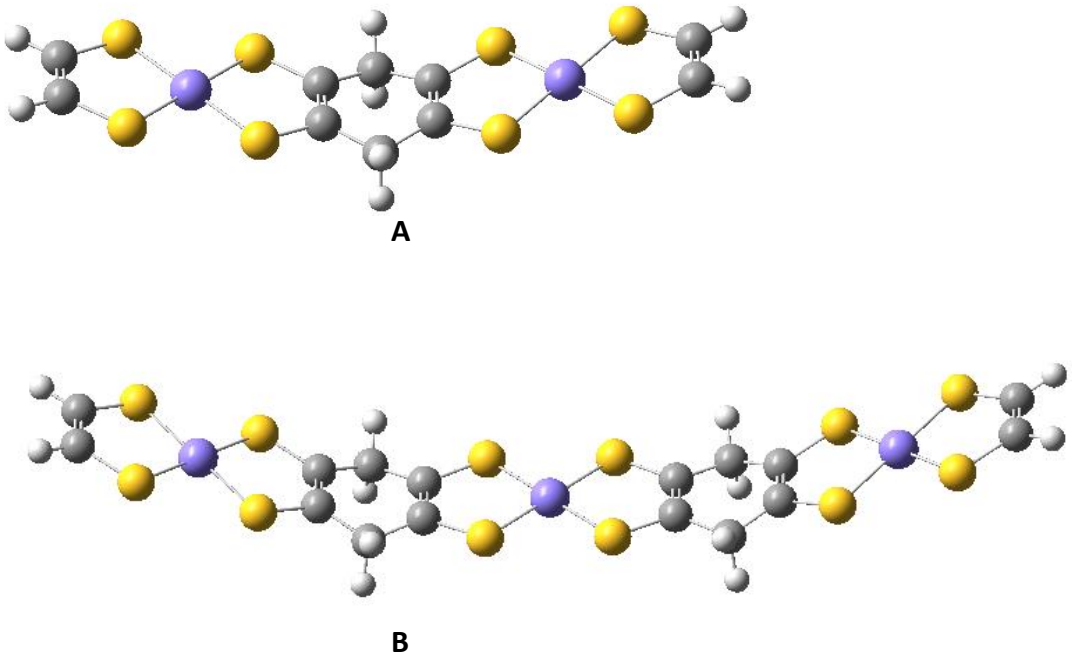

Figure S3 Structures of NiBDT-C_2H_4-NiBDT (A) and $(NiBDT)_3$-$(C_2H_4)_2$ (B), optimized with B3LYP/6-31G* method in the gas phase. Grey, yellow, and white atoms depict carbon, sulfur, and hydrogen, respectively.

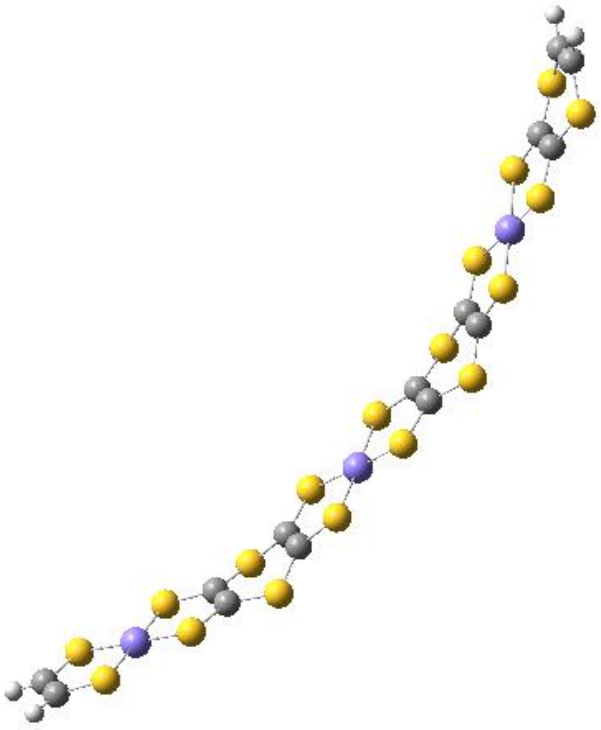

Figure S4. The structure of $C_{14}H_4Ni_3S_{12}S_6$ (II; Figure 3), optimized with B3LYP/6-31G* method in the gas phase. Grey, yellow, and white atoms depict carbon, sulfur, and hydrogen, respectively.

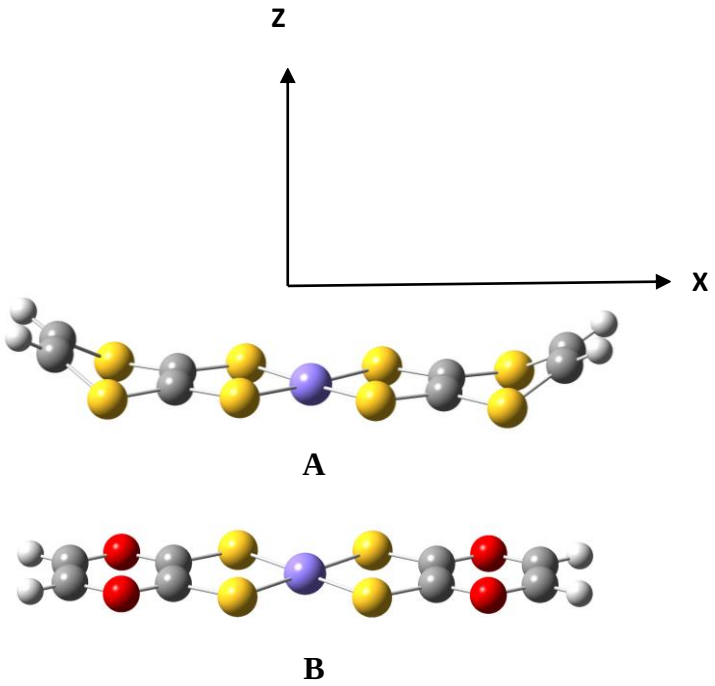

Figure S5. Structures of $C_8S_4NiS_4H_4$ (A) and $C_8O_4NiS_4H_4$ (B), optimized with B3LYP/6-31G* method in the gas phase. Grey, yellow, red and white atoms depict carbon, sulfur, oxygen and hydrogen, respectively.

Table S1. Basis set study of the second hyper polarizability of $(B\text{-}NiBDT)_2$. All the values were computed at the B3LYP/6-31G* geometry.

Method/Basis	$\gamma_{xxxx} x10^{-5}$/a.u.
(U)CAMB3LYP/SDD(Ni)/6-31G*	570
(U)CAMB3LYP/6-311G(2d)[a]	634
(U)CAMB3LYP/6-311+G*[a]	496
(U)CAMB3LYP/6-311G*[a]	698
(U)ωB97X/SDD(Ni)/6-31G*	899
(U)ωB97X/6-311G*[a]	1053
(U)BHandHLYP/SDD(Ni)/6-31G*	327
(U)BHandHLYP/6-311G*[a]	338

[a] All electron basis set.

TABLE S2. Description of excitations, computed with (U)CAM-B3LYP/6-31G* method.

B –NiBDT 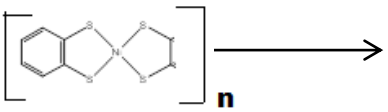						
State / **n**	**FDAET[a]**	**5**	**11**	**42**	**49**	**53**
1	HOMO(↑)-> LUMO(↑) (55%) (HOMO-6)(↑)-> LUMO(↑) (20%) (HOMO-5)(↓)-> LUMO(↓) (20%)	(HOMO-1)(↓)-> LUMO(↓) (81%)		(HOMO-15)(↑)-> LUMO(↑) (26%) HOMO(↑)-> (LUMO+4)(↑) 14%) (HOMO-1) (↑)-> (LUMO+3) (↑) (7%) (HOMO)(↓)-> (LUMO+5)(↓) (15%) (HOMO)(↓)-> (LUMO+3)(↓) (7%)	(HOMO-3)(↑)-> (LUMO+1)(↑) (40%) (HOMO-2)(↓)-> (LUMO+1)(↓) (47%)	(HOMO-1)(↑)-> (LUMO+3) (17%) (HOMO)(↓)-> (LUMO+3)(↓) (17%) (HOMO)(↓)-> (LUMO+5)(↓) (17%) (HOMO-1)(↓)-> (LUMO+4)(↓) (9%)
2	(HOMO-1)(↑)-> LUMO(↑) (69%) (HOMO-1)(↑)-> (LUMO+1)(↑) (11%)		(HOMO-11)(↑)-> (LUMO+1(↑) (7%) (HOMO-1)(↓)-> LUMO(↓) (76%)			
3	(HOMO-2)(↑)-> LUMO(↑) (39%) (HOMO-2)(↑)-> (LUMO+1)(↑) (10%) (HOMO-2)(↓)-> LUMO(↓) (20%)					
4	(HOMO-3)(↑)-> LUMO(↑) (22%) (HOMO-3) (↓)-> LUMO(↓) (28%)					

5	HOMO-3(↑)-> LUMO(↑) (22%) HOMO-3(↓)-> LUMO(↓) (22%) HOMO-5(↑)-> LUMO+1(↑) (6%) HOMO-5(↓)-> LUMO+1(↓) (6%) HOMO-3(↑)-> LUMO+1(↑) (4.5%) HOMO-3(↓)-> LUMO+1(↓) (4.5%)					
6	HOMO-3(↑)-> LUMO(↑) (17)%) HOMO-3(↓)-> LUMO(↓) (17)%) HOMO-3(↑)-> LUMO+1(↑) (4%) HOMO-3(↓)-> LUMO+1(↓) (4%) HOMO-6(↑)-> LUMO+1(↑) (5%) HOMO-6(↓)-> LUMO+1(↓) (5%) HOMO-6(↑)-> LUMO+1(↑) (6%) HOMO-6(↓)-> LUMO+1(↓) (6%)					

[a] This state is associated with the first dipole-allowed electronic transition (FDAET).